Implementation of Extremum Seeking Control in an Experimental Lab-Rig ⋆

Jose Matias * **Frida Bakken Myrvang** * **Johannes Jäschke** *

* *Chemical Engineering Department, Norwegian University of Science and Technology, Sem Sælandsvei* 4*, Kjemiblokk* 5*, Trondheim, Norway*

Abstract: Extremum seeking control (ESC) is an adaptive control method that can be used for production optimization. In the standard ESC approach, the process optimum is found by slowly adapting the inputs based on plant gradient approximations. Since ESC "learns" the system characteristics online using only plant measurements, it requires an appropriate time-scale separation between the system response, the excitation signal used for gradient approximation, and the dynamics to be optimized. Krishnamoorthy et al. (2019) proposed a dynamic ESC that identifies a local linear dynamic model using transient measurements and uses this model for computing the plant gradients. Consequently, the time-scale separation between the system response and the excitation signal is not required and the scheme converges to the optimum faster than the standard ESC. Albeit attractive, some practical challenges have been identified, such as gradient computation and constraint handling. The main contribution of this paper is to investigate how to overcome these challenges in a more realistic setting, in which dynamic ESC is implemented on a lab-scale plant that emulates a subsea oil well network. We compare the performance of two gradient computation approaches and present a constraint handling strategy for the system of interest, where multiple units compete for limited resources. The results show that dynamic ESC is able to drive the system to its optimum without constraint violations.

Keywords: Real-time Optimization; Extremum Seeking Control; Practical implementation

1. INTRODUCTION

In chemical industries, economic optimization is typically addressed by *Real-time optimization* (RTO) (Darby et al., 2011), where an economic criterion is maximized (e.g. profit) while satisfying operational and quality constraints. The most common RTO approach is the two-step RTO (Chen and Joseph, 1987). Here, the parameters of a rigorous steady-state model are estimated online and the updated model is used for finding the input values that maximize the economic performance.

If an accurate model is available and an appropriate algorithm is used for solving the optimization problems, two-step RTO can improve the plant economic performance significantly (Darby et al., 2011). However, obtaining such models can be complicated, time-demanding, and a continuous task, since the system most likely will change over time (Matias and Jäschke, 2021). Also, the model often represents an oversimplification of the process, and its predictions can differ significantly from the actual system behavior due to plant-model mismatch, uncertainty in parameters, and unmeasured disturbances. The calculated inputs are then optimal for the model, but not necessarily for the plant (Marchetti et al., 2009). Moreover, solving rigorous models online is computationally expensive and prone to numerical instabilities (Quelhas et al., 2013).

For addressing these issues, model-free optimization methods, like Extremum Seeking Control (ESC), can be used. ESC is an unconstrained optimization technique, where the gradients of the objective function with respect to the inputs are estimated implicitly or explicitly from measurements. The process is then optimized by driving the estimated gradients to zero using a control scheme. However, only few ESC applications have been reported in chemical processes, e.g.: wastewater chemical treatment (Martínez, 2007), and de-ammonification process (Trollberg, 2011).

The need to estimate the gradients is one of the main causes for the few practical applications. Chemical process tend to be slow and subject to unmeasured disturbances. Since ESC optimizes the *static* behavior of the system, we need to reach steady-state before estimating the gradients. If data from different plant conditions is used for estimating the gradients, the optimality of the computed inputs is affected (Krishnamoorthy et al., 2019). Even if the gradients are accurately estimated, the computed stationary points may no longer be optimal if a disturbance occurs while ESC is driving the plant to the desired condition (Trollberg and Jacobsen, 2013).

Krishnamoorthy et al. (2019) proposed a dynamic ESC that identifies a linear dynamic model using transient measurements and uses it for local steady-state gradient estimation. Consequently, this scheme tries to move towards the optimum also during transients, which improves the dynamic response to disturbances as well as the convergence speed to the desired condition. Both characteristics are attractive for industrial applications, especially in chemical processes. In this paper, we implemented the dynamic ESC on a lab-scale plant. The lab rig emulates a

⋆ The authors acknowledge financial support from the Norwegian Research Council, SUBPRO, grant number: 237893.

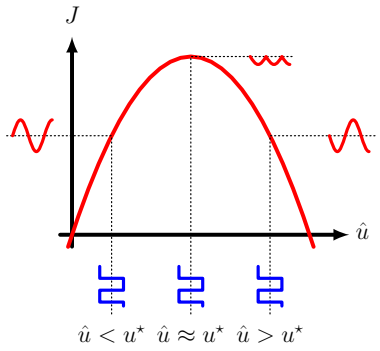

Fig. 1. Example of standard static ESC for an objective function J. Adapted from Brunton and Kutz (2019).

gas lift subsea oil well network, where the production optimization objective is to maximize the total oil production while accounting for multiple wells competing for limited gas lift injection.

The main contributions of the paper are: 1. the first application of the new dynamic ESC scheme in an real, physical system; 2. the development and implementation of a constraint handling strategy for the problem of interest. This is essential for practical applications since ESC is traditionally an unconstrained optimization method; 3. studying how the gradient estimation method works in a real system, which is typically not done in the literature. These contributions are important for investigating potential implementation issues, and give some intuition on how some design decisions affect the overall performance of dynamic ESC.

2. EXTREMUM-SEEKING CONTROL

In ESC schemes for production optimization, we use the system inputs u to maximize (or minimize) an economic objective function J without modeling their relationship. The basic idea is shown in Fig. 1. It consists of perturbing u periodically and measure the effect in J. The goal is to probe the slope of the objective function around a particular value of u. Then, based on the response pattern (e.g. if u increases, J decreases) and magnitude ($\Delta J/\Delta u$), we track the optimal input value u that corresponds to the peak of the objective function J. An interesting property of ESC schemes is that they are able to track the peak if the relation between u and J changes slowly with time.

Krstic and Wang (2000) provided a rigorous assessment of the stability of this ESC scheme. The main assumptions are that the static relationship between J and u has a unique local maximum (or minimum), and the system presents an appropriate time-scale separation between its response (the settling time after changing u), the input perturbation dynamics, and the optimum tracking. The reason is that, for proper identification of the static relationship between J and u, the plant needs to stabilize much faster than the periodic perturbation frequency. In turn, the optimum tracking must happen in the slowest time scale because the influence of the disturbances in the static map needs to be "averaged out" before adapting the inputs.

2.1 Dynamic Extremum-seeking control

If the principle of time scale separation holds, it is relatively straightforward to implement ESC (Tan et al., 2010). However, process plants are usually slow with settling times of hours. Hence, the requirement that the optimum tracking is carried out in a time scale much slower than the system response leads to ESC schemes that have prohibitive convergence speed (Krishnamoorthy et al., 2019). One alternative to avoid this drawback is to use a dynamic ESC approach, where transient measurements are used for identifying the relationship between the inputs u and the objective function J. In this case, the time scale separation between the system response and the periodic perturbation can be disregarded. Consequently, the required time scale difference between the system dynamics and the optimum tracking decreases significantly.

To this end, Krishnamoorthy et al. (2019) proposed a dynamic ESC that uses transient measurements to identify online a linear dynamic model around the current operating point. A scheme illustrating the method is shown in Fig. 2. Here, the steady-state gradients J_u are computed using the identified model as opposed to estimating them implicitly as in Fig. 1. Next, a simple control structure can be used to drive the gradients to the desired setpoint; for example, 0 if the optimization problem is unconstrained. However, if the optimization problem of interest is constrained, a constraint handling strategy needs to be developed. Additionally, since we need to identify models online, it is necessary to provide sufficient excitation to the system. Otherwise, there is not enough information to estimate the linear model parameters, especially near steady-state. Thus, it is always necessary to apply excitation signals (dithers) to the system.

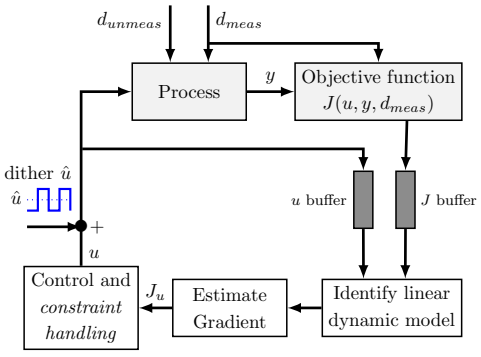

Fig. 2. Schematic of the Dynamic ESC approach proposed by Krishnamoorthy et al. (2019).

3. CASE STUDY

The experimental rig emulates a subsea oil well network. In the actual system, oil is extracted from reservoirs under the seabed to the top facilities on the sea level. The driving force for fluid flow is the reservoir natural pressure. In some cases, however, this pressure is not high enough and an artificial lifting method needs to be used. Among the options, gas lift injection is widely used due to its relatively low cost and robust design (Amara, 2017).

In gas lifted systems, compressed gas is injected at bottom of the well. Consequently, both the fluid bulk density as

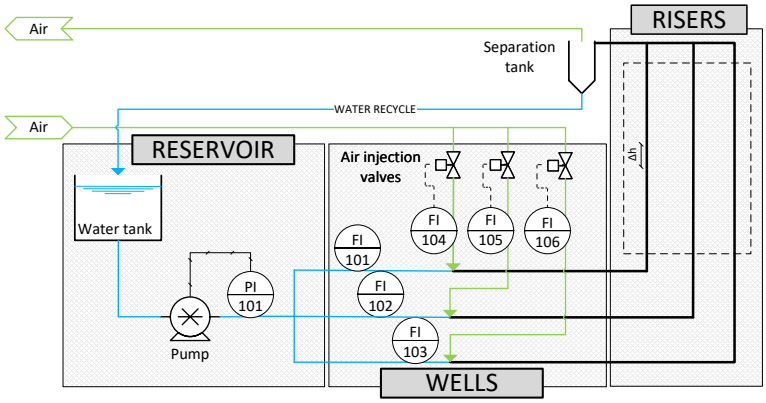

- **Inputs** $\boldsymbol{u} = [Q_{gl,1}, Q_{gl,2}, Q_{gl,3}]^T$
  air injection valves (FI104/105/106) setpoints
- **Measurements** $\boldsymbol{y} = [Q_{l,1}, Q_{l,2}, Q_{l,3}]^T$
  liquid flowrates (FI101/102/103)
- **Pump outlet pressure (PI101)**:
  fixed during experiments using a PI controller
- **Flowline material**:
  - water
  - air
  - air liquid mixture

Fig. 3. Experiment schematic.

well as the hydrostatic pressure exerted by the mixture at the reservoir outlet decrease. Since the reservoirs typically lie at depths of 300 to 2.000 meters, the change in the hydrostatic pressure has a significant effect on the reservoir back pressure, increasing the well production. However, if the gas injection rate is too big, the frictional pressure drop increases, dominates the hydrostatic pressure effect, and decreases the well production. For maximizing the system throughput, this trade-off needs to be considered.

ESC approaches are potential candidates for this task. First, the relationship between gas injection (input u) and the total production (objective function J) resembles the profile shown in Fig. 1. Second, most of the currently used production optimization methods is based on manually controlling the marginal gas-oil rate (i.e. J_u). Thus, ESC only automates the current procedures, which can increase its acceptance in industry (Pavlov et al., 2017).

3.1 Experimental Rig

The lab rig represents a gas-lifted network with 3 wells (Fig. 3). In the setup, water and air are used instead of oil and gas. Although different fluids are employed, the gas lift effect can still be seen and, consequently, the production optimization problem can be studied.

The setup has three main sections, reservoir, wells, and risers. The reservoir consists of a tank, a centrifugal pump, and a pressure sensor at the pump outlet. The pump rotation is regulated such that its outlet pressure is fixed at 1.285 bar. The wells are represented by three parallel hoses of 1.5 m with an inner diameter of 2 cm. Air is injected by three air flow controllers in the range of 1 to 5 $sL/min/well$. The setpoints of these controllers are the system inputs u, which are used for maximizing the system production. This system configuration leads to well liquid flowrates ranging from 2 to 20 $L/min/well$. The risers are composed of 2.2 m high hoses with the same diameter as in the well. After the riser, gas is vented out to the atmosphere and the liquid recirculated to the tank.

3.2 Production optimization problem

The optimal economic operation point is found by maximizing the liquid production "revenue" while considering the "cost" of gas lift compression. The optimization problem is subject to constraints g on gas injection bounds (Q_{gl}^L and Q_{gl}^U) and maximum gas availability ($Q_{gl}^{\max}$):

$$\max_{\mathbf{u}=[Q_{gl,1},Q_{gl,2},Q_{gl,3}]^T} J := \sum_{i=1}^{3} \alpha_{l,i} Q_{l,i} - \alpha_{gl} \sum_{i=1}^{3} Q_{gl,i}$$
$$\text{s. t.} \qquad (1)$$
$$\mathbf{g} := \begin{cases} Q_{gl,1} + Q_{gl,2} + Q_{gl,3} \leq Q_{gl}^{\max} \\ Q_{L,gl} \leq Q_{gl,i} \leq Q_{U,gl} \quad i = 1,2,3 \end{cases}$$

where, $Q_{l,i}$ is the liquid flowrate and $Q_{gl,i}$ is the gas lift injection of well i. The optimal gas injection $u^\star$ is implemented as the setpoint of the air flow controllers.

Table 1. Parameters values

Description	Symbol	Value
Max. gas lift availability	$Q_{gl}^{\max}$	7.5 sL/min
Gas injection lower bound	$Q_{L,gl}$	1 sL/min
Gas injection upper bound	$Q_{U,gl}$	4 sL/min
Well productivity index	α_l	[5, 10, 20] ($\$ \times min)/L$
Gas lift compression cost	α_{gl}	1 ($\$ \times min)/sL$

4. DYNAMIC ESC IMPLEMENTATION

4.1 Linear model identification and gradient estimation

For estimating the gradients, we first collect a buffer of N data points of the objective function, $\mathbf{J} = [J(1) \dots J(N)]$ and the input, $\mathbf{U} = [\mathbf{u}(1)^T \dots \mathbf{u}(N)^T]^T$, where N is newest and 1 the oldest sample. Next, we use the measurements in the buffer to identify an ARX model in the following form (for simplicity, we show the single-input/single-output case):

$$A_{poly}(q)J(t) = B_{poly}(q)u(t - n_k) + e(t)$$
$$\text{where } A_{poly}(q) = 1 + a_1 q^{-1} + \dots + a_{n_a} q^{-n_a} \qquad (2)$$
$$B_{poly}(q) = b'_1 + \dots + b'_{n_b} q^{-n_b+1}$$

in which, q^{-1} is the unit delay operator, n_a is the number of poles, n_b is the number of zeros, and n_k is the dead time. In our implementation, we estimate the coefficients a's and b's online but choose the ARX model structure offline by defining n_a, n_b, and n_k beforehand. Then, the

steady-state gradient around the current operating point can be computed by:

$$J_u = A_{poly}^{-1} B_{poly} \tag{3}$$

4.2 Control and constraint handling

After calculating the estimated steady-state gradients, we use a control structure to drive J_u (controlled variable - CV) to the desired setpoints (SP) by changing Q_{gl} (manipulated variable - MV). In an unconstrained case, the CVs can be simply controlled to a constant set-point of zero. Since our case is constrained, we have to integrate a constraint handling strategy to the controller block for determining these SPs.

Our strategy, which is summarized in Fig. 4, was developed based on the first-order conditions of optimality (FOC) of Eq. (1). By re-arranging the constraints to $\mathbf{g}(\mathbf{u}) \leq 0$, we can define the Lagrangian of Eq. (1) as:

$$\mathcal{L}(u, \lambda) = -J(u) + \lambda^T \mathbf{g}_{\mathcal{A}}(u) \tag{4}$$

where, λ are the KKT multipliers (note that we want to maximize the objective function). The first order conditions of optimality can then be written as:

$$\begin{aligned} \nabla_u \mathcal{L}(u^\star, \lambda^\star) = -\nabla_u J(u^\star) + \nabla_u \mathbf{g}_{\mathcal{A}}(u^\star)^T \lambda^\star = \mathbf{0} \\ \mathbf{g}_{\mathcal{A}}(u^\star) = \mathbf{0} \end{aligned} \tag{5}$$

in which, $\mathbf{g}_{\mathcal{A}}$ denotes the active set for a given scenario. Due to the nature of the problem of interest, the maximum gas lift capacity is *always* active at the optimum (Krishnamoorthy et al., 2019). If this is the only active constraint (i.e. $\mathbf{g}_{\mathcal{A}} := g_{Q_{gl}^{max}}$), we obtain from Eq. (5):

$$\nabla_u J(u^\star) = [1,\ 1,\ 1] \lambda^\star_{Q_{gl}^{max}} \tag{6}$$

We can then expand $\nabla_u J(u^\star)$:

$$[J_{u_1}(u^\star),\ J_{u_2}(u^\star),\ J_{u_3}(u^\star)] = [1,\ 1,\ 1] \lambda^\star_{Q_{gl}^{max}} \tag{7}$$

Then, by substituting $\lambda^\star_{Q_{gl}^{max}}$ and rearranging, we have:

$$J_{u_i}(u^\star) - J_{u_j}(u^\star) = 0 \quad \forall i \neq j \tag{8}$$

Thus, by enforcing equality of the gradients, we fulfill the FOC in the case where only the maximum gas lift capacity is active. Based on this principle, we first assume that only the maximum gas lift capacity Q_{gl}^{max} is active and, then, enforce the bound constraints afterwards. The constraint handling strategy is then given by:

(i) Find the input with the largest magnitude. Denote this input u_1. This will be used later for controlling the active constraint Q_{gl}^{max}.
(ii) Treat the problem as if only Q_{gl}^{max} is active. Use control to drive $\hat{J}_{u_1}$ to the smallest possible value and use the other inputs for guaranteeing gradient equality as in Eq. (8). Check the gradient order to make sure that the inputs with largest gradients are increased.
(iii) Enforce bound constraints by clipping the inputs.
(iv) Check the maximum gas lift capacity constraint. If it is feasible, implement. Otherwise, go to step (v).

If infeasible, we enforce Q_{gl}^{max} constraint by setting:

$$u_1 = Q_{gl}^{\max} - (u_2 + u_3) \tag{9}$$

However, this can lead to two issues: (a) u_1 is decreased, even if J_{u_1} is the largest gradient, or (b) u_1 lower bound is violated. Thus, a certain amount ϕ must be subtracted from u_2 and u_3 before enforcing Eq. (9).

(v) For determining ϕ, we check J_{u1} and J_{u_2}:
  (a) If $J_{u_1} < J_{u_2}$, then u_1 can be decreased. However, the lower bound $Q_{L,gl}$ on u_1 should not be violated:
  $$\phi = (u_2 + u_3) - (Q_{gl}^{\max} - Q_{L,gl})$$
  (b) If $J_{u_1} \geq J_{u_2}$, then u_1 should not be decreased:
  $$\phi = (u_2 + u_3) - (Q_{gl}^{\max} - u_1)$$
  Since $J_{u_2} > J_{u_3}$ (Step (ii)), ϕ is subtracted from u_3. However, u_3 lower bound should not be violated. In this case, the remaining part of ϕ_{rem} is subtracted from u_2. Next, we compute Eq. (9) and implement.

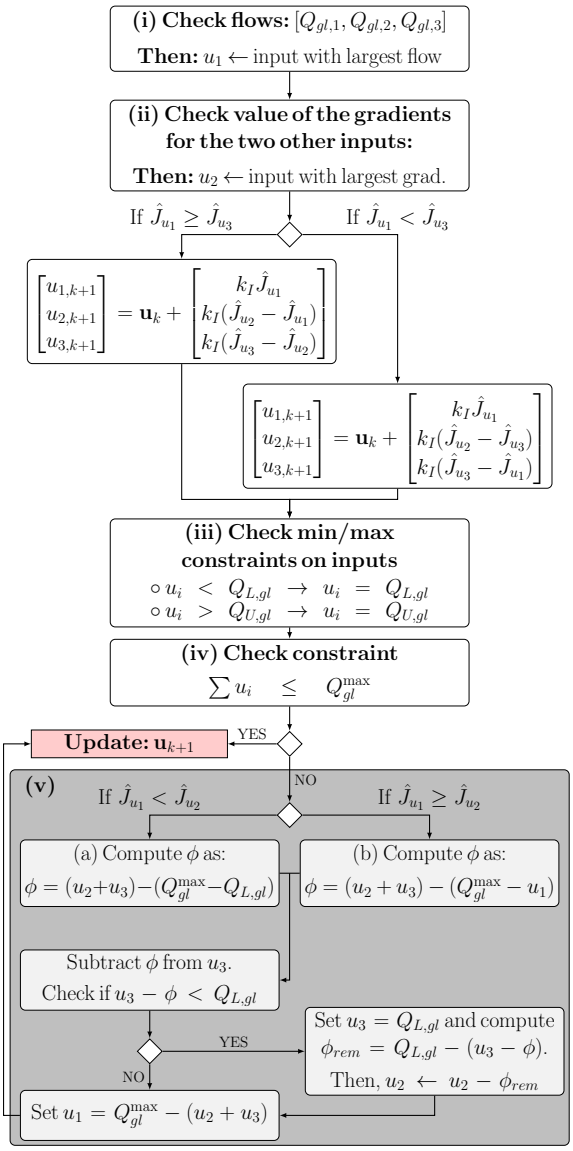

Fig. 4. Flow diagram for the constraint handling

Remark: Note that we do not treat the MV bound constraints rigorously. They also have associated KKT multipliers λ that should be considered. However, our strategy guarantees feasibility of the MV constraints, which are typically prioritized over other constraints in real applications. Moreover, the proposed strategy enforces the total capacity constraint in accordance with Krishnamoorthy et al. (2019).

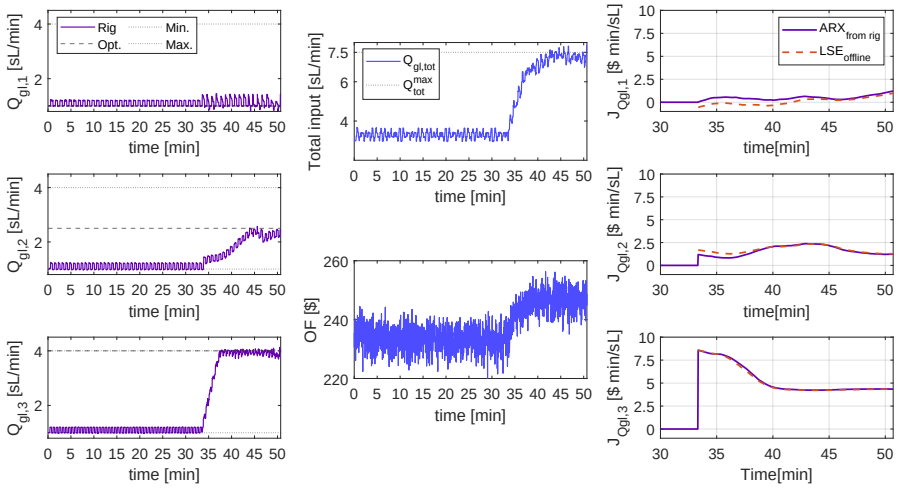

Fig. 5. Result of the optimization of the gas lifted well network using ARX. The figure shows the inputs, objective function, the total input usage, and the estimated gradients. The gradients were compared offline with the estimates obtained by the technique proposed by Hunnekens et al. (2014) referred to as LSE.

4.3 Dither

In order to have enough information for identifying the ARX model online, a dither must be added to each of the three inputs $\mathbf{u}_{k+1}$ for exciting the system. We use a periodic square wave as a dither. This type of dither is used in the lab rig because it is easy to implement, and improves the convergence speed of the ESC approach when compared to the sinusoidal dither (Tan et al., 2008). The inputs with the added dither can be written as:

$$\hat{\mathbf{u}}_{k+1} = \mathbf{u}_{k+1} + \begin{bmatrix} a_1 \ \text{sq.wave}(\omega_1)_k \\ a_2 \ \text{sq.wave}(\omega_2)_k \\ a_3 \ \text{sq.wave}(\omega_3)_k \end{bmatrix} \tag{10}$$

where a_i are the amplitudes of the dither signals, and ω_i the frequencies of the square wave.

4.4 Tuning parameters

Since the inputs are of the same nature (gas flow rates), the dither amplitudes are chosen to be the same. They should be chosen large enough such that their effect on the objective function can be clearly identified. However, unnecessarily large input perturbations should be avoided. The frequencies must have different values in order to differentiate the individual effects of the inputs in the objective function. We choose small control gains k_I for slowing down control actions, and a large buffer length N to increase the information content for the ARX model identification. For avoiding oscillations due to noisy gradient estimates, we apply a moving average filter using a sliding window of length N_{maf} in the CV before calculating the MVs (in step (ii) of Fig. 4).

5. EXPERIMENTAL RESULTS AND DISCUSSION

The results of the system optimization using dynamic ESC are shown in Fig. 5. The left side plots show the three inputs, which are the gas lift rates. On the middle column, we show the total gas lift injection, constrained by $Q_{gl}^{\max}$, and the objective function value J. The plots on the right side present the gradients of the objective function with respect to the inputs. Since the real values of the gradients are unknown, the gradients computed online using the ARX model are compared with an offline estimation based on a technique proposed by Hunnekens et al. (2014), referred as LSE. In this technique, a 1^{st} order least-squares fit model is identified at every sampling time and used for gradient estimation. The goal of this comparison is to check if the estimated gradients are reasonable or not.

Table 2. Dynamic ESC Tuning parameters

Description	Symbol	Value
Controller sampling time	t_s	2 s
Buffer length	N	900 data points
Moving average	N_{maf}	100 data points
Dither amplitude	a	0.1 sL/min
Dither frequency	ω	[1/60, 1/50, 1/40] s^{-1}
Controller gain	k_I	0.005 $sL^2/(\$ \times min^2)$
Order of polynomial $A(q)$	n_a	3
Order of polynomial $B(q)$	n_b	[2 2 2]
ARX time delay	n_k	[0 0 0]

Although the optimal operation cannot be rigorously calculated, we can use engineering intuition to determine if the optimization approach behaves as expected. Due to the weights in J, $\alpha_3 > \alpha_2 > \alpha_1$, we expect $Q_{gl,3}$ to be on the upper bound ($4sL/min$) and $Q_{gl,1}$ on the lower bound ($1sL/min$). Since $Q_{gl}^{\max}$ should be active at the optimum, $Q_{gl,2}$ can be easily calculated. In the experiment, the inputs start from an arbitrary suboptimal point, $\mathbf{u} = [1,1,1]^T$ sL/min. The control initiates after 33 minutes of operation due to N and N_{mean} and drives the inputs to the predicted value. However, around 45 minutes there is a deviation in the expected behavior. For a short time period $\hat{J}_{u_2} > \hat{J}_{u_3}$ and, according to the diagram in Fig. 4, u_2 ($Q_{gl,1}$) should be increased and u_3 ($Q_{gl,2}$) decreased. This unwanted behavior happens most likely due to unmeasured disturbance in the rig; however, dynamic ESC is able to reject it and track the optimum again. From the objective function perspective, there is no visible loss as a consequence of this disturbance.

Regarding the gradient estimation, the computed values are coherent with the objective function weights (i.e.

$J_{Q_{gl,3}} > J_{Q_{gl,2}} > J_{Q_{gl,1}}$). As $Q_{gl,3}$ goes to the optimum, $J_{Q_{gl,3}}$ decreases, as expected, and then stabilizes. In turn, J_{u1} and J_{u3} present some small oscillation. However, since $J_{Q_{gl,2}} > J_{Q_{gl,3}}$ most of the time, there is no significant effect on the overall performance. By comparing the different gradient estimation techniques, ARX and LSE have similar results except in the initial period. The main reason is the presence of transient information. In LSE, the system needs to behave as a static map. Even though the time constants of the rig are fast due to small pipe holdups, abrupt changes in the inputs that happen after the control starts dominate the system dynamics. However, after the inputs tend to their stationary values, the gradient estimated values are consistent.

Finally, the constraints are not violated during the experiment, which shows that the constraint handling strategy worked. Additionally, it did not seem to affect the gradient estimation for the ARX and LSE, since there is no significant effect after the bound constraints on $Q_{gl,1}$ and $Q_{gl,3}$ become active. In Myrvang (2021), the strategy has been implemented together with dynamic ESC in the same system, but with different disturbance scenarios. It also had good results, showing flexibility. However, it may require adaptation for specific disturbance scenarios that have not been considered.

6. CONCLUSIONS

In this paper we discussed two practical challenges for dynamic ESC implementations: constraint handling and gradient estimation. We developed an *ad-hoc* constraint handling strategy for the system of interest (Fig. 4). Moreover, the experimental results indicated that the strategy works since dynamic ESC was able to drive the system to its optimum without violating the constraints. When it comes to the different gradient estimation techniques, ARX and LSE had similar performances. LSE worked well in the system because the lab rig dynamic response is fast. In systems where the dynamic transitions play an important role, ARX is expected to have a better performance, since ARX is a time series model.

In addition to the challenges listed above, a clear drawback of ESC implementations is the significant number of parameters that have to be tuned. Although there are some vague guidelines in the literature, this is a demanding task. The parameters affect each other and the task becomes even harder if the system has several inputs. Furthermore, even though we are using a dynamic ESC, in which the convergence is faster, we had to choose parameter values that led to a very slow and smooth operation. Specifically, the controller gains k_I and the CV moving average N_{mean}. Otherwise, the overall performance would be strongly affected by the noisy objective function measurements. Hence, in the tuning stage, there is a clear trade-off between economic performance and stability that should be properly addressed. Another drawback is the need to apply a dither to the inputs. The constant input oscillation is usually not desired in chemical systems and may be associated with safety risks. However, if we can show that ESC can be reliably implemented and systematically improve the economic performance of different systems while guaranteeing a safe operation, it could be possible to convince plant operators and engineers to implement ESC in real chemical systems.

REFERENCES

Amara, A.B. (2017). Gas lift: past and future. In *Society of Petroleum Engineers - SPE Middle East Artificial Lift Conference and Exhibition 2016*, 420–425.

Brunton, S.L. and Kutz, J.N. (2019). *Data-driven science and engineering: Machine learning, dynamical systems, and control*. Cambridge University Press.

Chen, C.Y. and Joseph, B. (1987). On-line optimization using a two-phase approach: An application study. *Industrial and Engineering Chemistry Research*, 26(9), 1924–1930.

Darby, M.L., Nikolaou, M., Jones, J., and Nicholson, D. (2011). RTO: An overview and assessment of current practice. *Journal of Process Control*, 21(6), 874–884.

Hunnekens, B.G.B., Haring, M.A.M., Van de Wouw, N., and Nijmeijer, H. (2014). A dither-free extremum-seeking control approach using 1st-order least-squares fits for gradient estimation. In *53rd IEEE Conference on Decision and Control*, 2679–2684. IEEE.

Krishnamoorthy, D., Ryu, J., and Skogestad, S. (2019). A dynamic extremum seeking scheme applied to gas lift optimization. *IFAC-PapersOnLine*, 52(1), 802–807.

Krstic, M. and Wang, H. (2000). Stability of extremum seeking feedback for general nonlinear dynamic systems. *Automatica*, 36(4), 595–602.

Marchetti, A., Chachuat, B., and Bonvin, D. (2009). Modifier-adaptation methodology for real-time optimization. *Industrial and Engineering Chemistry Research*, 48(13), 6022–6033.

Martínez, E. (2007). Extremum-seeking control of redox processes in wastewater chemical treatment plants. In *Computer Aided Chemical Engineering*, volume 24, 865–870. Elsevier.

Matias, J. and Jäschke, J. (2021). Online model maintenance in real-time optimization methods. *Computers and Chemical Engineering*, 145, 107141.

Myrvang, F.B. (2021). *Implementation of Extremum Seeking Control in an Experimental Lab-Rig*. Master's thesis, NTNU.

Pavlov, A., Haring, M., and Fjalestad, K. (2017). Practical extremum-seeking control for gas-lifted oil production. In *2017 IEEE 56th Annual Conference on Decision and Control (CDC)*, 2102–2107. IEEE.

Quelhas, A.D., de Jesus, N.J.C., and Pinto, J.C. (2013). Common vulnerabilities of RTO implementations in real chemical processes. *Canadian Journal of Chemical Engineering*, 91(4), 652–668.

Tan, Y., Moase, W.H., Manzie, C., Nešić, D., and Mareels, I.M.Y. (2010). Extremum seeking from 1922 to 2010. In *Proceedings of the 29th Chinese control conference*, 14–26. IEEE.

Tan, Y., Nešić, D., and Mareels, I. (2008). On the choice of dither in extremum seeking systems: A case study. *Automatica*, 44(5), 1446–1450.

Trollberg, O. and Jacobsen, E.W. (2013). Multiple stationary solutions to the extremum seeking control problem. In *2013 European Control Conference (ECC)*, 376–381. IEEE.

Trollberg, O. (2011). Extremum seeking control applied to a deammonification process. Technical report.